

Interband Electro-Optical Properties of Germanium. I. Electroabsorption*

YOSHIHIRO HAMAKAWA,† F. A. GERMANO,‡ AND PAUL HANDLER

*Department of Physics, Materials Research Laboratory and Department of Electrical Engineering,
University of Illinois, Urbana, Illinois*

(Received 17 July 1967)

In this and in the following paper, we report on the effect of an electric field on interband optical transitions in germanium. We have measured the electroabsorption effect on the direct edge of germanium at three different temperatures: 14, 83, and 300°K. The amplitude of the signal increases fivefold from the highest to the lowest temperature. Analysis of the temperature and electric-field dependence of data show that there is very little relationship between the data and the predictions of one-electron band theory (Franz-Keldysh effect). It will be shown that the Coulomb interaction (the exciton and its continuum of states) is probably responsible for most of the observed behavior at both low and high temperatures.

I. INTRODUCTION

A SERIES of theoretical papers¹⁻⁷ culminating in the work of Aspnes⁸ has developed expressions for the change in the interband optical properties of a solid with the application of an electric field. These theoretical papers have always assumed the one-electron approximation and predict that the change in the imaginary part of the dielectric constant, $\Delta\epsilon_2$, will be oscillatory near critical points in the Brillouin zone. Experimental results in both electroabsorption and electroreflectance have borne out the oscillatory nature of these predictions in a qualitative way and led investigators to believe that the Coulomb interaction between the electron and hole could be neglected. A quantitative comparison of theory and experiment has not been accomplished because it requires knowledge of the magnitude of the electric field and avoidance of thermal-broadening effects. To determine whether the one-electron approximation is appropriate, we report on the line shape of $\Delta\epsilon_2$ at the direct edge in germanium at 14°K. We will show that the data do not agree with predictions of one-electron band theory and that the Coulomb interaction must be included, not only for the bound states (the exciton) but also for the continuum. Although Duke and Alferieff⁹ have considered

the effect of the Coulomb interaction on the bound states, the binding energies in germanium are so small, ~ 1 meV, that even at the smallest fields used (3×10^8 V/cm) the bound states and the continuum are strongly mixed. In the past it has been suggested that results obtained from *p-n* junctions¹⁰⁻¹² might be spurious. In this paper we have used both single crystals and *p-n* junctions and the results obtained are identical.

II. EXPERIMENTAL

Two types of germanium samples containing very thin windows in their centers were used in this experiment. One was an abrupt *p-n* junction where the window thickness was 20–25 μ , and the second was a nearly intrinsic (*n*-type 30–40 Ω cm) single-crystal wafer with a 10- μ -thick window. For the preparations of both these samples, various techniques known to give uniform and shiny surfaces were utilized. The optical transmission was measured at each step of etching to control the sample thickness. The specimens were initially square wafers with a 7×7 mm² area with a thickness of 100 μ . A rectangular window with dimensions 2×4 mm² and desired thickness was made in the center of the wafer by a combination of masking and chemical etching. The samples were mounted on germanium substrate with a window to avoid strain effects at low temperatures, and then set into a liquid-helium optical Dewar schematically shown in Fig. 1. A PbS detector was mounted on the liquid-nitrogen shield directly behind the sample. To obtain good ohmic contact to single-crystal germanium, 5-at.% Sb-doped semitransparent gold film was evaporated on both sides of the wafer in a layer about 50 Å thick.

The modulation techniques used to yield the field-induced differential absorption coefficient $\Delta\alpha(\omega, \mathcal{E})$ from measurement of the quantities ΔI (field-modulated signal) and I (total intensity of light) have been de-

* This work was supported in part by the Advanced Research Projects Agency under Contract No. SD-131 and by the U. S. Army Research Office (Durham).

† Present address: Faculty of Engineering Science, Osaka University, Toyonaka, Osaka, Japan.

‡ Fellow of the Conselho Nacional de Pesquisas (Brazil). Present address: Instituto de Fisica, Universidade do Ceara, Fortaleza, Brazil.

¹ W. Franz, *Z. Naturforsch.* **13a**, 484 (1958).

² L. V. Keldysh, *Zh. Eksperim. i Teor. Fiz.* **34**, 1138 (1958) [English transl.: *Soviet Phys.—JETP* **7**, 788 (1958)].

³ J. Callaway, *Phys. Rev.* **130**, 549 (1963); **134**, A998 (1964); **143**, 564 (1966).

⁴ K. Tharmalingam, *Phys. Rev.* **130**, 2204 (1963).

⁵ C. M. Penchina, *Phys. Rev.* **138**, A924 (1965).

⁶ M. Chester and L. Fritsche, *Phys. Rev.* **139**, A518 (1965).

⁷ Y. Yacoby, *Phys. Rev.* **A263** (1965).

⁸ D. E. Aspnes, *Phys. Rev.* **147**, 554 (1966); **153**, 972 (1967). Note in the second paper that the definition of the quantity B has an extra factor of c in the denominator.

⁹ C. B. Duke and M. E. Alferieff, *Phys. Rev.* **145**, 583 (1966).

¹⁰ A. Frova, P. Handler, F. A. Germano, and D. E. Aspnes, *Phys. Rev.* **145**, 575 (1966).

¹¹ Y. Hamakawa, F. A. Germano, and P. Handler, *J. Phys. Soc. Japan*, Suppl. **21**, 111 (1966).

¹² P. Handler, *Phys. Rev.* **137**, 1862 (1965).

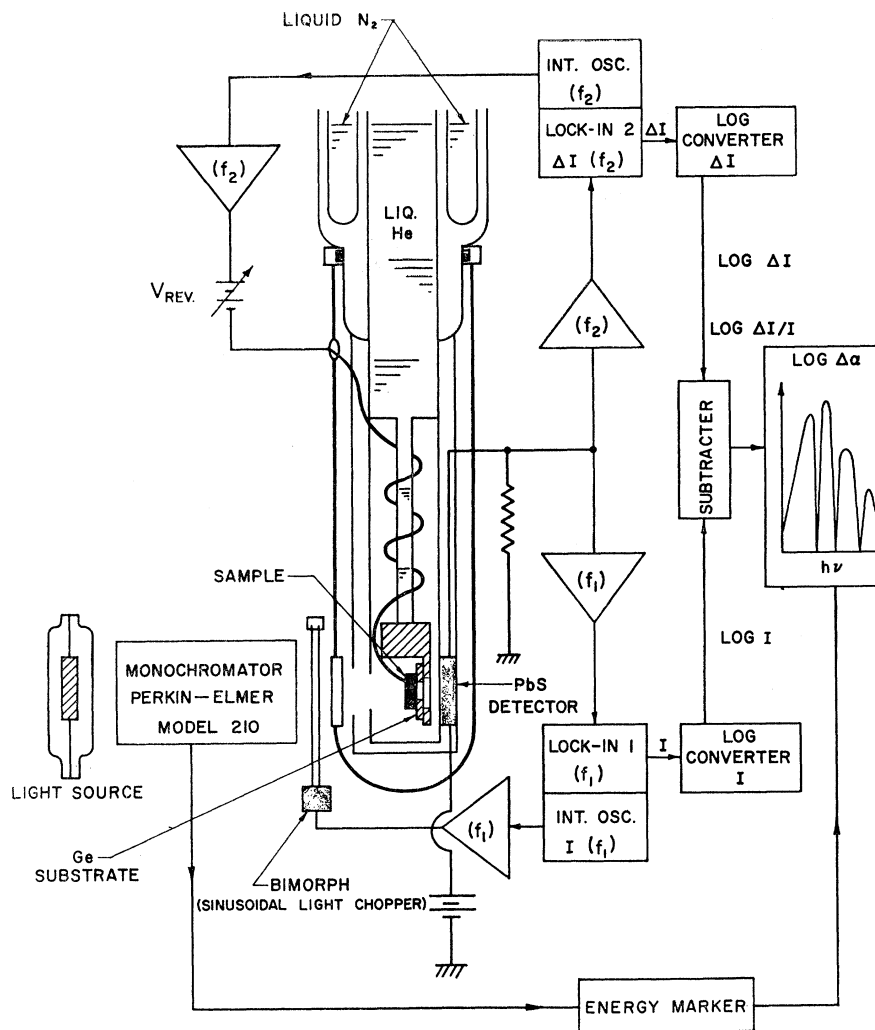


FIG. 1. Schematic diagram of the experimental setup used for measurements of the differential absorption coefficient at low temperatures.

scribed previously both for the p - n junction and single crystal.¹⁰⁻¹³

The block diagram of the measurement system used is also shown in Fig. 1. In the figure the lock-in 1 for detecting I was a PAR model JB-5 and the lock-in 2 for ΔI was a model HR-8. A Perkin Elmer model 210 monochromator was employed with a grating of 640 lines/mm. As a light source, a Sylvania quartz iodine (Sun Gun) lamp was used. The resolution of 0.5 meV was sufficient for the observation of line structures. For the detection of signal I , a small known fraction ($\sim 5\%$) of beam was chopped sinusoidally by a Bimorph chopper with a frequency of $f_2=90$ cps. The electric-field modulating frequency was $f_1=1500$ cps at room temperature and at the low temperatures $f_1=500$ cps because of the slower response of the PbS cell.

To obtain the ratio $\Delta I/I$ directly, the output of two Moseley Autograph logarithmic converters (model 60D) were connected so that the dc output of the

lock-in amplifiers was transformed into $[\log \Delta I - \log I] = \log[\Delta I/I]$. For the p - n junction experiments the amplitude of the modulating ac voltage ΔV was chosen so as to keep the ratio of the maximum electric field in the junction \mathcal{E} , to ΔV constant for all runs. In that way, the recorded signal gives directly $\Delta\alpha(\omega, \mathcal{E})$ with the same proportionality constant in the same scale for all runs in the case of a p - n junction.¹⁰⁻¹²

$$\ln[\Delta\alpha(\omega, \mathcal{E})] = \ln(\Delta I/I) + \ln(\mathcal{E}/\Delta V). \quad (1)$$

III. DISCUSSION AND RESULTS

Although the data will be presented in terms $\Delta\alpha$, the change in the absorption coefficient, this discussion will be in terms of $\Delta\epsilon_2$, the imaginary part of the dielectric function. For the direct edge in germanium they are simply related by

$$\Delta\alpha = (\omega/nc)\Delta\epsilon_2. \quad (2)$$

¹³ T. S. Moss, J. Appl. Phys. Suppl. 32, 2136 (1961).

Aspnes, Handler, and Blossey¹⁴ have shown that $\epsilon_2(\omega, \mathcal{E})$ for an M_0 edge as derived by many authors³⁻⁸ can be rewritten in a simple convolution form of zero-field density of states as

$$\epsilon_2(\hbar\omega, \mathcal{E}) = \frac{B}{\omega^2} \int_{E_g}^{\infty} \left(\frac{E - E_g}{\hbar} \right)^{1/2} \left[\frac{1}{\hbar\Omega} \text{Ai} \left(\frac{E - \hbar\omega}{\hbar\Omega} \right) \right] dE, \quad (3)$$

where $\Omega^3 = (e\mathcal{E})^2 / 8\mu\hbar$, B is a constant which contains the dipole matrix element, and ω is the frequency of the incident photon. In the limit of zero electric field ($\mathcal{E} \rightarrow 0$), $\Omega \rightarrow 0$ and

$$\lim_{\Omega \rightarrow 0} \left(\frac{1}{\hbar\Omega} \right) \text{Ai} \left(\frac{E - \hbar\omega}{\hbar\Omega} \right) = \delta(E - \hbar\omega). \quad (4)$$

Equation (3) reduces to the form

$$\lim_{\Omega \rightarrow 0} \epsilon_2(\hbar\omega, \mathcal{E}) = \epsilon_2(\hbar\omega, 0) = \frac{B(\hbar\omega - E_g)^{1/2}}{\omega^2 \hbar}, \quad \hbar\omega \geq E_g. \quad (5)$$

Substituting the second equality of Eq. (5) into Eq. (3) we have

$$\epsilon_2(\hbar\omega, \mathcal{E}) = \frac{1}{(\hbar\omega)^2} \int_{E_g}^{\infty} E^2 \epsilon_2(E, 0) \left(\frac{1}{\hbar\Omega} \right) \text{Ai} \left(\frac{E - \hbar\omega}{\hbar\Omega} \right) dE. \quad (6)$$

The change in ϵ_2 with field $\Delta\epsilon_2$ can then be written in the compact form

$$\Delta\epsilon_2(\hbar\omega, \mathcal{E}) = \frac{1}{(\hbar\omega)^2} \int_{E_g}^{\infty} E^2 \epsilon_2(E, 0) \times \left[\left(\frac{1}{\hbar\Omega} \right) \text{Ai} \left(\frac{E - \hbar\omega}{\hbar\Omega} \right) - \delta(E - \hbar\omega) \right] dE. \quad (7)$$

The functional form of $\Delta\epsilon_2$ is plotted on an arbitrary

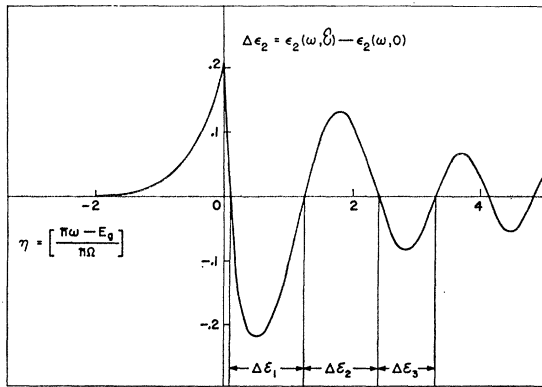


FIG. 2. $\Delta\epsilon_2(\omega, \mathcal{E})$ of Eq. (7) in arbitrary units plotted versus the dimensionless variable η .

¹⁴ D. E. Aspnes, P. Handler, and D. Blossey, Phys. Rev. **166**, 921 (1968),

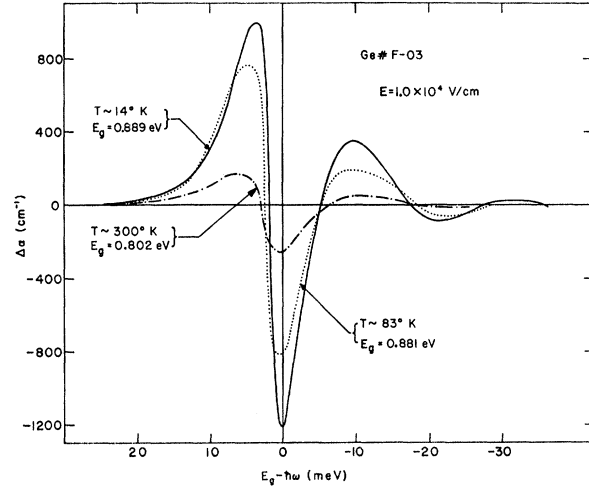


FIG. 3. Field-induced change in the absorption coefficient for the electric field 1×10^4 V/cm taken at three different temperatures.

scale in Fig. 2 as a function of the dimensionless variable

$$\eta = (\hbar\omega - E_g) / \hbar\Omega, \quad (8)$$

which depends upon the energy distance from the gap as well as the magnitude of the electric field to the $\frac{2}{3}$ power as contained in Ω . This equation is valid as long as the reduced effective mass of the electron-hole pair, μ , and the matrix element for the transition are constant over a large range of energy. Before discussing the data it might be worth listing the predictions of this one-electron theory. The results shall be discussed in terms of $\Delta\alpha$ since for these experiments at the direct edge ω and n in Eq. (2) can be assumed essentially constant.

(1) The energy gap should occur very close to first positive peak,

$$\eta = \frac{\hbar\omega - E_g}{\hbar\Omega} = 0,$$

as shown in Fig. 2.

(2) The amplitude of the peaks in $\Delta\alpha$ should increase as $\mathcal{E}^{1/3}$. The peak heights should never decrease with increasing electric field.¹⁵

(3) The relative amplitudes of the various peaks should increase in a fixed ratio.

(4) For energies below the gap, $\hbar\omega < E_g$, the asymptotic form for $\Delta\alpha$ becomes

$$\Delta\alpha(\omega, \mathcal{E}) = \alpha(\omega, \mathcal{E}) - \alpha(\omega, 0) = \frac{K\mu}{\omega(E_g - \omega)} \exp \left[-\frac{4(2\mu)^{1/2}(E_g - \omega)^{3/2}}{3\hbar\epsilon\mathcal{E}} \right], \quad (9)$$

where K is a constant. Then rewriting and taking the

¹⁵ This point is seen more clearly when $\Delta\epsilon_2$ is written in the form Eqs. (13b) and (14) of Aspnes's paper (Ref. 8) where the $\mathcal{E}^{1/3}$ dependence appears explicitly in the $\theta^{1/2}$ term.

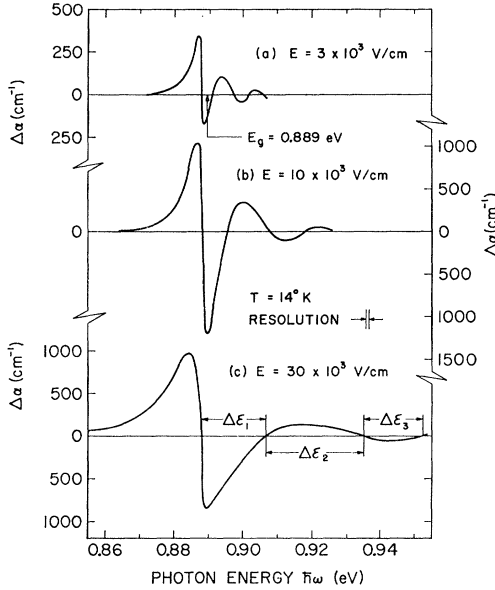


FIG. 4. The change in absorption coefficient, $\Delta\alpha(\omega, \mathcal{E})$, at 14°K for three different fields.

logarithm of both sides we have

$$\ln[\omega(E_g - \hbar\omega)\Delta\alpha(\omega, \mathcal{E})] = -\frac{4(2\mu)^{1/2}(E_g - \hbar\omega)^{3/2}}{3\hbar c\mathcal{E}} + \ln K\mu. \quad (10)$$

Thus knowledge of E_g , \mathcal{E} , and $\Delta\alpha$ as a function of ω allows a determination of the effective mass from the slope analysis of a plot of Eq. (10).

(5) The amplitude of the peaks on the high-energy side should decrease slowly with η .

(6) Last and perhaps most important is that for the function $\Delta\epsilon_2$, the distance between peak heights in energy units or the distance between zeros in energy units should increase according to $\mathcal{E}^{2/3}$.

We will now compare the data with the six predictions given above. Figure 3 shows the temperature dependence of $\Delta\alpha$ at three different temperatures but for the same electric field. The curves have been superimposed on a common energy scale where the energy gap at each temperature is taken to be zero. We note that the energy gap as determined by Macfarlane¹⁶ falls at the center of the negative peak rather than at the first zero. The increase in amplitude of $\Delta\alpha$ between 300 and 14°K is a factor of 5. The 300°K result can be considered as thermal broadening of the low-temperature results. The problem has recently been discussed by Enderlein¹⁷ and by Aspnes⁸ for Lorentzian broadening. The two higher-temperature curves can be approximately fitted

¹⁶ G. G. Macfarlane, T. P. McLean, T. E. Quarrington, and V. Roberts, Phys. Rev. Letters **2**, 252 (1959).

¹⁷ R. Enderlein, Phys. Status Solidi **20**, 295 (1967); R. Enderlein and R. Keiper, *ibid.* **19**, 673 (1967).

by Lorentzian broadening of the 14°K curve with a broadening parameter roughly proportional to temperature. However, the Lorentzian-broadened theoretical curve given in Eq. (7) cannot be used to fit the data even when the energy gap is chosen as a free parameter. Either the low-energy tail or the last two half-oscillations can be matched, but not both, and in neither case is the first negative peak ever matched. The results of an attempt at such a fit can be seen in Fig. 5, Ref. 11.

Figure 4 shows the values of $\Delta\alpha$ for three different values of the electric field. In Fig. 4 we see that the energy gap as determined by Macfarlane¹⁶ lies above the first positive peak in all cases. Figure 5 shows the dependence of the amplitude of the first three peaks on the applied electric field. Not only do they increase too quickly, i.e., faster than $\mathcal{E}^{1/3}$, but the first negative peak does not follow the other two. It increases faster at low field and decreases still faster at higher fields. We shall show later that the behavior of the first negative peak is qualitatively what one would expect from a weakly bound exciton and its continuum states.

In Fig. 4(c) we have denoted three quantities $\Delta\epsilon_1$, $\Delta\epsilon_2$, and $\Delta\epsilon_3$ which are differences in energy units of the zeros of the observed $\Delta\alpha$. If we let η_n be a zero of $\Delta\epsilon_2$, then from Eq. (8)

$$\eta_n - \eta_{n'} = \frac{2(\mu)^{1/3}[\hbar\omega_n - \hbar\omega_{n'}]}{(e\hbar)^{2/3}[\mathcal{E}^{2/3}]}, \quad (11)$$

$$\Delta\epsilon_n = \hbar\omega_n - \hbar\omega_{n'} = (\eta_n - \eta_{n'}) \left[\frac{(e\hbar)^{2/3}}{2\mu^{1/3}} \right] \mathcal{E}^{2/3}, \quad (12)$$

so that a log-log plot of $\hbar(\omega_n - \omega_{n'})$ versus \mathcal{E} should yield a slope of $\frac{2}{3}$.

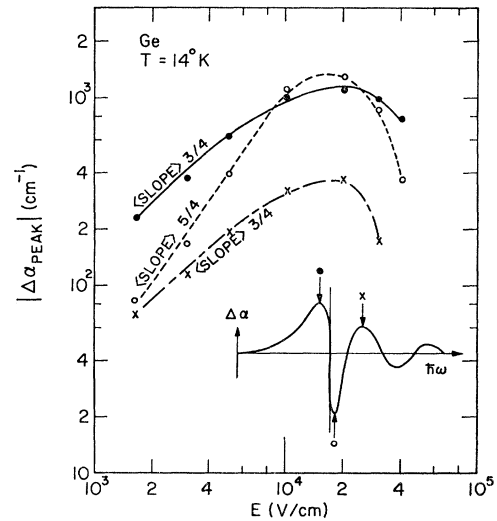


FIG. 5. The amplitude dependence of the first two positive and first negative peak as a function of the magnitude of the electric field.

Figure 6 shows that only $\Delta\epsilon_2$ and $\Delta\epsilon_3$ have the right field dependence and also the right magnitude, which is determined from the expected values of the reduced mass where the light and heavy holes have been averaged.¹¹ $\Delta\epsilon_1$ does not have either the right slope or magnitude. The observed width of the negative peak is too narrow at all values of the electric field studied. A similar analysis could have been carried out using peak-to-peak differences. We have used the zeros because attempts to fit the experimental $\Delta\alpha$ with a Lorentzian-broadened $\Delta\epsilon_2$ function of Eq. (7) showed that the $\Delta\epsilon$'s discussed here were relatively insensitive to the amount of broadening. Figure 6 also shows that the single-crystal results at lower field agree very well with the p - n junction data at higher fields.

Finally, Fig. 7 shows that $\Delta\epsilon_2$ is relatively temperature-independent, whereas $\Delta\epsilon_1$, the width of the first negative peak, is temperature-dependent, becoming narrower at lower temperatures.

Another indication of the difficulty of fitting the data is shown by taking the ratios of the $\Delta\epsilon_n$'s at two temperatures. The ratio of the oscillation period $\Delta\epsilon_{nT}/\Delta\epsilon_{nT'}$ measured at two different temperatures T and T' but at the same electric field should, according to Eq. (12), be proportional to $(\mu_T/\mu_{T'})^{1/3}$. Using for the electron effective mass¹⁸ $m_e^* = 0.036m$ at 300°K, and 0.041 m at 4.2°K, and for the light and heavy hole masses¹⁹ $m_L^* = 0.0426m$ and $m_H^* = 0.376m$, the ratio between room temperature 4.2°K should be 1.03. This value is found to be very close to the experimentally observed ratio for $\Delta\epsilon_2$ between 300 and 14°K. On the other hand, the value of $\Delta\epsilon_1$ varies with temperature as shown for the solid lines in Fig. 7, and the ratio of the $\Delta\epsilon_1$'s by

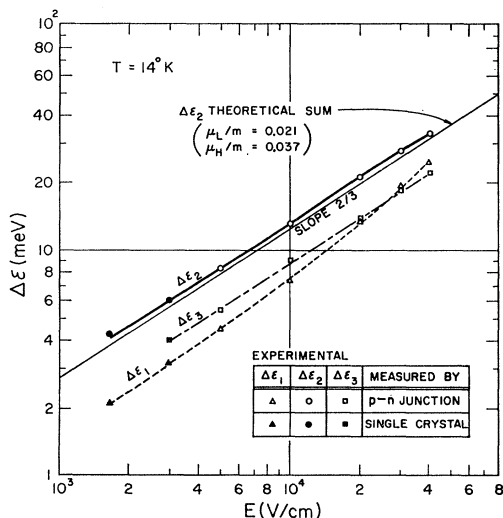


FIG. 6. Electric-field dependence of the width of the half-oscillations above the direct edge in energy units taken at 14°K.

¹⁸ S. Zwerdling, B. Lax, and L. M. Roth, Phys. Rev. **108**, 1402 (1957).

¹⁹ R. N. Dexter, H. Y. Zeiger, and B. Lax, Phys. Rev. **104**, 637 (1956).

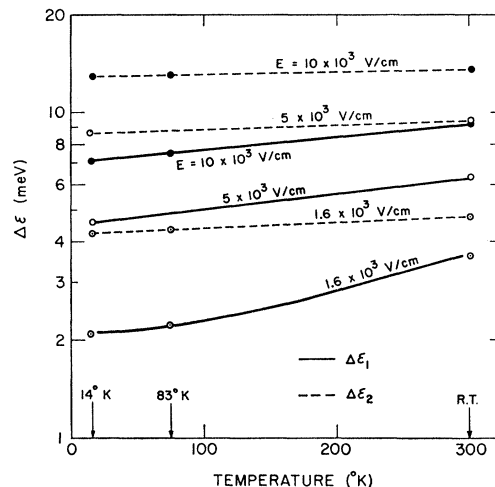


FIG. 7. Temperature dependence of $\Delta\epsilon_1$ and $\Delta\epsilon_2$ at various electric fields.

the same temperatures is more than 1.7 for electric fields of 3×10^3 V/cm.

Analysis of the exponential tail of $\Delta\alpha(\omega, \mathcal{E})$ by means of Eq. (10) can determine an effective reduced mass of the electron-hole pair, μ_{eff} . Values of $\mu_{\text{eff}} = 0.024m$ at 14°K and 0.022 m at room temperature were obtained. These values are very close to those calculated from the values of m_e^* , m_L^* , and m_H^* mentioned above. Inserting these effective reduced masses into the relation we also obtained $[\mu(14^\circ\text{K})/\mu(300^\circ\text{K})]^{1/3} = 1.03$. Although this last point is in agreement with Eq. (10) it is also in agreement with the predictions of an exponential tail on the low-energy side of an exciton peak as predicted by Duke and Alferieff.⁹ An analysis of the data which assumes that both the effective mass and the energy gap are unknown has been reported by Frova and Penchina.²⁰ Using a method of analysis similar to theirs we find that the data predict an E_g too low from the known value by a few meV. We also note that the oscillatory peaks on the high-energy side where the Coulomb interaction is weak fall off in amplitude much faster than that shown in Fig. 2. Even if the curve of Fig. 2 is Lorentzian broadened to give agreement within the $\Delta\epsilon_3$ energy region the peaks still fall off more sharply than predicted. See Fig. 5 of Ref. 11.

At 14°K analysis of the amplitude of the first peak on the assumption that Eq. (7) is valid showed that the square of the dipole matrix element is 1.2 atomic units. This value is very close to the value of 1.24 calculated from the pseudopotential method²¹ and 1.06 estimated from the data in McLean's paper.²²

In conclusion, we observe that the six predictions of the one-electron theory are only partially observed

²⁰ A. Frova and C. M. Penchina, Phys. Status Solidi **9**, 767 (1965).

²¹ F. H. Pollak and C. Cardona, J. Phys. Chem. Solids **27**, 423 (1966); Phys. Rev. **142**, 530 (1966).

²² T. P. McLean, Progr. Semicond. **5**, 53 (1960).

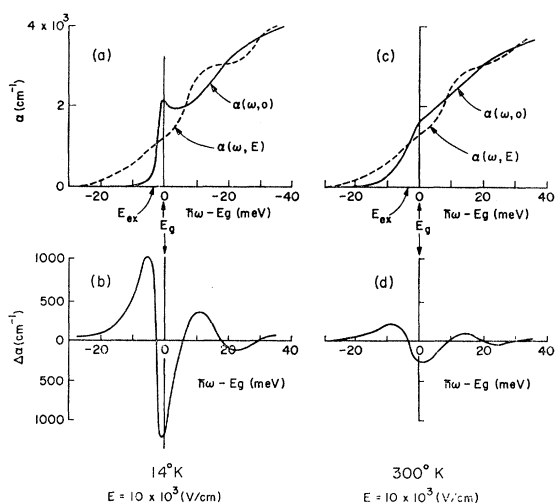


FIG. 8. Schematic representation of the electroabsorption near the direct edge.

in the data. The few measures of agreement such as μ_{eff} do not differentiate between a one-electron and an exciton theory. The agreement of the field dependence of $\Delta\epsilon_2$ and $\Delta\epsilon_3$ with the theory does not provide much additional confirmation. But in the next paper,²⁸ it will be shown that this field dependence will be very useful in the evaluation of the magnitude of the effective fields in the electroreflectance spectra.

IV. EXCITON AND CONTINUUM STATES

The observed line shapes can be simply although only qualitatively understood if it is assumed that they

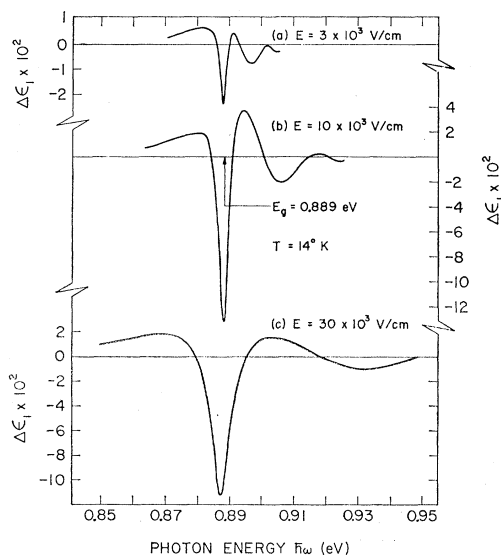


FIG. 9. $\Delta\epsilon_1(\omega, E)$ as obtained from Kramers-Kronig analysis of the data of Fig. 4.

²⁸ Y. Hamakawa, P. Handler, and F. Germano, following paper, Phys. Rev. **167**, 709 (1968).

result from the interaction of the quenching of the exciton oscillator strength and the electric-field broadening of its continuum states. We assume that even in the presence of the Coulomb interaction, Eq. (6) represents an approximately correct functional form for $\epsilon_2(\omega, E)$, where $\epsilon_2(E, 0)$ is now the experimentally observed zero-field dielectric function. The validity of this assumption is doubtful and in fact wrong when the exciton absorption line is completely separate from its continuum. Nonetheless we will use Eq. (6), for illustrative purposes only, to describe the temperature and field dependence of the electroabsorption data. The solid lines of Figs. 8(a) and 8(c) are the zero-field data of Macfarlane¹⁶ and Glass.²⁴ Figures 8(b) and 8(d) are the observed electroabsorption data plotted on the exact same energy scale. The matching is better than 0.5 meV. Also, there has been no adjustment of amplitude. The dashed lines of Figs. 8(a) and 8(b) are the result of a simple addition of the two curves to show α in the presence of an electric field. In this model, the first negative peak is associated with the quenching of the exciton whereas the first two positive peaks can be considered as arising from the broadening of the exciton peak. Data of this type have already been obtained by Vrehen²⁵ at low fields, and these measurements extend his results to higher fields. This model explains why the first negative peak narrows at low temperature (see behavior of $\Delta\epsilon_1$ in Fig. 7). It also explains the amplitude behavior shown in Fig. 5. At low electric fields the exciton is quenched and the negative peak amplitude rises sharply. There is no interference from the continuum states since the electric field is too small to mix states distant in energy to $\Delta\epsilon_2$ at the exciton energy. See also Fig. 3 of Ref. 11. As the field increases Eq. (6) indicates that there will always be a positive $\Delta\alpha$ contribution at the exciton energy from the continuum states. At very highest fields the contribution from the continuum at the exciton energy is then greater than that due to the quenching of the exciton and in addition a general broadening sets in which reduces the amplitude of all the peaks.

This interaction of the continuum and the exciton is seen most clearly in the indirect absorption edge of silicon. See Fig. 3 of Ref. 10. In this case the oscillator strength of the exciton is much weaker than that of the continuum and for very moderate fields the negative peak completely disappears. There remains only one large positive peak which represents the only region in which there is constructive interference between the bound and unbound states.

Since many investigators are measuring the electroreflectance of germanium at low temperatures, we plot, in Fig. 9, $\Delta\epsilon_1(\omega, E)$ at 14°K for three different values of the field. Since the field is uniform and its magnitude is known, these curves should be useful for comparing

²⁴ A. M. Glass, Can. J. Phys. **43**, 12 (1965).

²⁵ Q. H. F. Vrehen, Phys. Rev. **145**, 675 (1966).

electroreflectance data taken under conditions where the magnitude of the field is unknown.

V. CONCLUSIONS

We have shown that the predictions of the one-electron theory are not obeyed by the data and that a theory which takes into account the Coulomb interaction is much more likely to describe the experimental observations.

ACKNOWLEDGMENTS

The authors are indebted to Dr. D. Aspnes and Dr. C. J. Hermanson for stimulating conversations, and they are grateful to D. F. Blossey for mathematical derivation of the broadened Airy integral. We also wish to thank J. McNatt and D. E. Cullen for their assistance in the course of the present work, and J. Swartz and the Delco Radio Company for their help in the sample preparation.

Interband Electro-Optical Properties of Germanium.

II. Electroreflectance*

YOSHIHIRO HAMAKAWA,[†] PAUL HANDLER, AND F. A. GERMANO[‡]

Department of Physics, Materials Research Laboratory and the Department of Electrical Engineering, University of Illinois, Urbana, Illinois

(Received 17 July 1967)

By modifying the experimental conditions of the semiconductor-in-electrolyte electroreflectance technique we have been able to obtain the flat-band condition at the surface and therefore obtain results which can be simply interpreted. In particular, it is shown that the Kramers-Kronig transforms of the electro-absorption experiments of the previous paper, where the field is known and uniform, agree quite well with our new electroreflectance data at the direct edge of germanium. The agreement between the two methods allows a direct determination of the effective electric field in the electroreflectance experiments. It is found that the effective electric field is directly related to the average penetration depth of the photons and therefore explains the increasing width of the electroreflectance lines with energy, observed in all previous experiments. Detailed analysis of the 2.1- to 2.3-eV peaks under these new experimental conditions shows that they are not necessarily the result of spin-orbit splitting and may arise from many different parts of k space.

I. INTRODUCTION

IN the previous paper,¹ we showed that the observed I line shape at the direct edge of germanium was mainly related to the quenching of the exciton oscillator strength and the electric-field broadening of the continuum states. It was also observed that there were two useful methods of analysis which do not depend upon whether or not the Coulomb interaction between the electron-hole pair is taken into account. The first is that the slope of the exponential tail will give a good indication of the effective mass involved, and the second is that the difference in the zeros of the oscillations in energy units increases with the electric field as the $\frac{2}{3}$ power. In this paper we will use these results to determine the effective electric field associated with electroreflectance spectra, and we shall also show that degeneracy of various critical points in the 2.0–2.3-eV

region makes it difficult to assign the two peaks observed by Cardona,² Seraphin,^{3,4} and Ghosh⁵ to any one point in k space.

II. ELECTROREFLECTANCE LINE SHAPE AT CRITICAL POINTS

Aspnes,^{6,7} and Aspnes, Handler, and Blossey⁸ have shown that for the four different types of critical points, six distinct line shapes are possible for $\Delta\epsilon_2(\omega, \mathcal{E})$ and, via the Kramer-Kronig relations, also six line shapes for $\Delta\epsilon_1(\omega, \mathcal{E})$. The six possible line shapes for $\Delta\epsilon_2(\omega, \mathcal{E})$ are

$$\Delta\epsilon_2(\omega, \mathcal{E}) = \left\{ \begin{array}{l} \pm AF(\pm\eta) \\ AG(\pm\eta) \end{array} \right\}. \quad (1)$$

² M. Cardona, K. L. Shaklee, and F. H. Pollack, *Phys. Rev.* **154**, 696 (1967), and references therein.

³ B. O. Seraphin, R. B. Hess, and N. Bottka, *J. Appl. Phys.* **36**, 2242 (1965); B. O. Seraphin and N. Bottka, *Phys. Rev.* **145**, 628 (1966).

⁴ B. O. Seraphin and R. B. Hess, *Phys. Rev. Letters* **14**, 138 (1965).

⁵ A. K. Ghosh, *Solid State Commun.* **4**, 565 (1966).

⁶ D. E. Aspnes, *Phys. Rev.* **147**, 554 (1966).

⁷ D. E. Aspnes, *Phys. Rev.* **153**, 972 (1967).

⁸ D. Aspnes, P. Handler, and D. Blossey, *Phys. Rev.* **166**, 921 (1968).

* This work was supported in part by the U. S. Army Research Office (Durham) and the Advanced Research Projects Agency under Contract No. SD-131.

[†] Present address: Faculty of Engineering Science, Osaka University Toyonaka, Osaka, Japan.

[‡] Fellow of the Conselho Nacional de Pesquisas (Brazil). Present address: Instituto de Fisica, Universidade do Ceara Fortaleza, Brazil.

¹ Y. Hamakawa, F. A. Germano, and P. Handler, preceding paper, *Phys. Rev.* **167**, 703 (1968).